21st Australasian Fluid Mechanics Conference
Adelaide, Australia
10-13 December 2018

Sound Generation by a Supersonic Reacting Mixing Layer

I. Cartmill[1], N. Gibbons[1], V. Wheatley[1] and C. Doolan[2]

[1]School of Mechanical and Mining Engineering
University of Queensland, St Lucia QLD 4072, Australia

[2]School of Mechanical and Manufacturing Engineering
University of New South Wales, Sydney NSW 2052, Australia

Abstract

Direct numerical simulation (DNS) is used to investigate the sound generation of a reacting, temporally-evolving hydrogen-air mixing layer with a convective Mach number of 0.7. Pressure data are collected on both sides of the mixing layer and analysed in the wavenumber domain to reveal the spectra and relative magnitudes of the sound propagated in the two fluid layers. By comparing with DNS analysis of an equivalent non-reacting flow, we also investigate the relative contribution of the turbulent heat release to the overall sound field generated by this supersonic mixing layer. Better understanding of the noise production mechanisms inside a scramjet engine will enable improved engine design to minimise and control potential risks to both airframe and sensitive instrumentation.

Introduction

Aero-acoustic loads inside a scramjet engine are largely uncharacterised and difficult to calculate, leading to concerns about the airframe fatigue life and vibration damage to onboard electronics [3]. The prediction and control of such loads is therefore a key technical challenge limiting our ability to design robust, and ideally reusable, hypersonic vehicles. Such vehicles are needed to develop a more reliable, flexible and economical space launch technology.

Various features of the flow through a scramjet engine contribute to the generation of sound. These include, *inter alia*, shock-boundary layer interactions, interactions between shocks and shear layers, turbulent velocity fluctuations, and the effects of combustion. The major component of direct combustion noise results from volume expansion caused by unsteady heat release. The combustion noise generated by supersonic reacting flows has not been extensively studied but is an important area of research in the prediction and control of aero-acoustic loads inside a scramjet engine. Here, we focus on sound generation in a canonical flow: a temporally-evolving supersonic hydrogen-air mixing layer.

If we can determine the extent to which the noise generated and propagated inside a scramjet engine can be attributed to different sources and affected by different flow features including, in the present case, supersonic turbulent mixing layer heat release and underlying fluid composition, we will be in a better position to implement strategies to control that noise in the design process.

Numerical Method and Flow Configuration

The simulations were performed using the UnStructured 3D (US3D) code [8], developed by Candler's group at the University of Minnesota, which solves the finite-volume formulation of the full compressible Navier-Stokes equations. US3D is capable of simulating hypersonic flows with implicit timestepping in complex geometries exhibiting strong shocks, turbulent shear layers, and non-equilibrium thermochemistry. It has previously been demonstrated that US3D, which is not a specialised aero-acoustics code, is capable of adequately resolving in a reacting supersonic flow the low-amplitude waves typically found in acoustics applications [4].

Gas chemistry is dealt with using the non-equilibrium hydrogen oxidation scheme of Jachimowski [6]. Thermal equilibrium gas modelling is used, based on the thermodynamic tables published in [7]. The inviscid fluxes are computed using a hybrid scheme designed for supporting LES/DNS simulations with strong shock waves and other discontinuities, comprising a low-dissipation symmetric term and a high-dissipation asymmetric term that is only active near discontinuities where more dissipation is required:

$$\mathbf{F}_f = \mathbf{F}_{sym} + \alpha_{diss}\mathbf{F}_{diss} \quad (1)$$

The symmetric term is from a 6th-order accurate gradient reconstruction method based on [13] and tested in [11]. The dissipative flux term is computed using the modified Steger-Warming method from [8], with the eigenvalues modified to remove the symmetric component. The switch α_{diss} which varies between 0 and 1 to control the presence of dissipation is computed using the method of [2]. The viscous terms are computed with a least-squares estimation of the gradients, and discretized using the method described in [8]. Implicit time advancement is via the Full-Matrix-Point-Relaxation method described in [15], modified for second order time accuracy by retaining the explicit fluxes from the previous step and blending them with those of the current step.

In the present work, a three-dimensional domain is created to model a region of interest surrounding the top surface of a hydrogen fuel plume a short distance downstream from a scramjet fuel injector. To reduce computational costs, we approximate the spatial evolution of this mixing layer with temporal evolution in a periodic domain. An illustration of the simulation geometry is shown in figure 1.

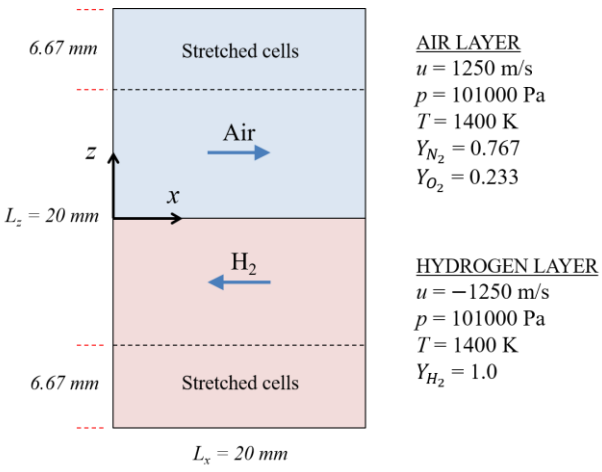

Figure 1. Mixing layer simulation domain and initial conditions.

Periodic boundary conditions have been implemented in the streamwise and spanwise directions. Stretched grid regions with symmetric boundary conditions are used to create non-reflecting outflows from the domain in the transverse direction. Discounting the regions of stretched cells, the dimensions of the modelled 3D space are $L_x = L_y = L_z = 20\,mm$. The domain is physically small due to the high computational cost of DNS.

The structured computational grid contains 28.6 million cells, and has been designed to adequately resolve both the Kolmogorov length scale η_k at which the smallest turbulent eddies are dissipated by viscosity, and the Batchelor length scale η_b at which molecular diffusion dominates fluctuations in scalar concentration. The average value of $\Delta x/\eta_k$ throughout the growing central mixing layer falls within the range 2 - 3.8 during both reacting and non-reacting simulations. The average value of $\Delta x/\eta_b$ is strictly smaller, falling in the range 1.2 - 2.3.

In order for turbulent combustion to occur during a short simulation, the chosen mean flow conditions depart somewhat from a typical scramjet flow. The velocity field is initialised with a streamwise convective velocity difference of $\Delta u = 2500\,m/s$ between the air flow in the top half of the domain and the hydrogen flow in the bottom half of the domain. This is a higher velocity difference than in a typical scramjet flow but enables a rapid transition to turbulence.

The convective Mach number [9, 10] for both streams is calculated as $M_c = \Delta u/(c_{air} + c_{H_2}) \approx 0.7$, where c represents the speed of sound in the relevant fluid, indicating that compressibility effects in the mixing layer are significant here.

The mean flow velocity varies between $\Delta u/2$ in the air flow and $-\Delta u/2$ in the hydrogen flow. The gas properties are blended at the interface between the two streams to initiate the evolution of the mixing layer. For each primitive variable $\psi = [Y_{N_2}, Y_{O_2}, Y_{H_2}, u]$, where Y is the relevant species mass fraction and u is the streamwise velocity component, the value is interpolated between the air and hydrogen sides using a hyperbolic-tangent profile as follows:

$$\psi = f\psi_{air} + (1 - f)\psi_{H_2} \tag{2}$$

$$f = \frac{1}{2}\tanh\left(\frac{6z}{\zeta}\right) + \frac{1}{2} \tag{3}$$

where z is the geometry coordinate in the transverse (inhomogeneous) direction, and $\zeta = 0.03 \times L_z$ is a smearing parameter that controls the initial thickness of the mixing layer.

The initial static pressure $p = 101\,kPa$ and temperature $T = 1400\,K$ for the air flow are realistic but at the higher end of the typical range [12]. In order to ensure rapid auto-ignition and robust combustion of the hydrogen during the simulation, and to compare sound propagation through the two layers under similar flow conditions, the hydrogen layer is also initialised with the same values of p and T.

The average kinematic viscosity ν of the fluid mixture across the centre of the mixing layer at the end of each simulation (reacting and non-reacting) together with the relative velocity Δu and the vorticity thickness δ_ω are used to calculate the Reynolds number of the flow:

$$Re_{\delta_\omega} = \frac{\Delta u\,\delta_\omega}{\nu} \tag{4}$$

The vorticity thickness is calculated as:

$$\delta_\omega = \frac{\Delta u}{\left(\frac{\partial \bar{u}}{\partial z}\right)_{max}} \tag{5}$$

where $\bar{u}$ is the average streamwise velocity and z is the transverse geometry coordinate.

At the end of the simulation, the flow reaches $Re_{\delta_\omega} \approx 12500$ in the case of the reacting mixing layer, and $Re_{\delta_\omega} \approx 13500$ in the non-reacting mixing layer. Typically, a fully-developed turbulent flow may be expected with $Re \geq 10000$ - 20000 [1].

Periodic Pressure Fluctuations

Visualizations of the instantaneous flow in the centre-plane of the reacting DNS are shown in figure 2. Figure 2(a) shows the water mass fraction within the hydrogen-air mixing layer at $Re_{\delta_\omega} \approx 7500$, shortly after transition to turbulence, demonstrating that robust combustion is occurring. Figure 2(b) shows the resulting pressure field surrounding the mixing layer at the same time point. Periodic pressure fluctuations indicative of sound generation are apparent in both the lower hydrogen layer and the upper air layer. Similar fluctuations appear in the non-reacting version of the simulation.

It can be seen that the pressure waves radiated into the two flows are quite different, primarily as a consequence of the very different speeds of sound in air ($\sim 751\,m/s$) and hydrogen ($\sim 2843\,m/s$). Configuring the simulation with equal and opposing flow velocities results in large central turbulent structures remaining almost stationary as the flow develops over time, although smaller turbulence scales do convect with the flow at larger distances from the central interface. Relative to these dominant structures, the air layer is travelling at $M \approx 1.7$. We therefore hypothesize that the broad strongly-directional pressure bands extending into the upper air layer in

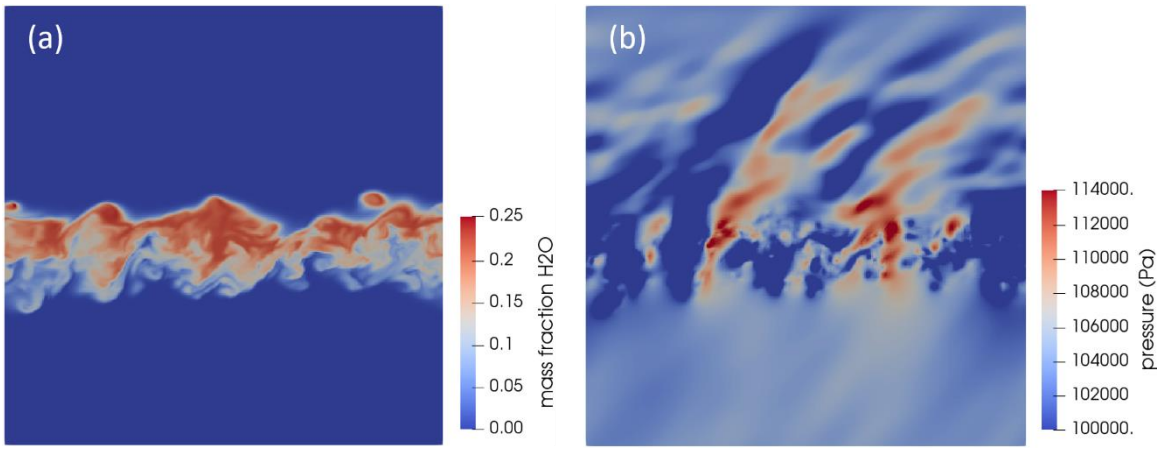

Figure 2. Simulated reacting flow field at $Re_{\delta_\omega} \approx 7000$ showing (a) H_2O mass fraction, and (b) surrounding pressure field.

figure 2(b) are near-field Mach waves, similar to those observed in supersonic jets [14], radiated by these large quasi-stationary turbulent eddies. The hydrogen layer on the other hand is flowing at only $M \approx 0.5$ relevant to the large-scale turbulent structures. The pressure fluctuations radiated down into that layer are therefore not characterised by the same strong pattern, as Mach wave emission becomes increasingly inefficient at subsonic speeds.

To investigate the unsteady pressure loading in both fluids, and in both reacting and non-reacting cases, we have analysed parallel slices through the 3D domain at equal distances ($8.5\ mm$) above and below the initial mixing layer location ($z = 0$). A wavenumber analysis was performed by computing the power spectral density (PSD) of the pressure signal along each streamwise row of cells in the selected slice, and averaging those PSD results across all rows. The resulting average PSD for each entire slice was then plotted for a set of time points across a Re_{δ_ω} range of approximately 1000. Figure 3 shows the PSD plots in the air and hydrogen layers for both reacting and non-reacting cases at different stages of the mixing layer evolution.

Sound Wave Coupling with Air and Hydrogen

Figure 3(a) shows the Mach number contours of the reacting flow at $Re_{\delta_\omega} \approx 8000$, still soon after the transition to turbulence and when the resulting pressure waves have reached the parallel observation slices in both fluid layers. It can be seen in figure 3(b) that the magnitudes of the pressure fluctuations in the air layer are markedly higher (up to 30 dB) than those in the hydrogen layer, for all wavenumbers. This suggests that the

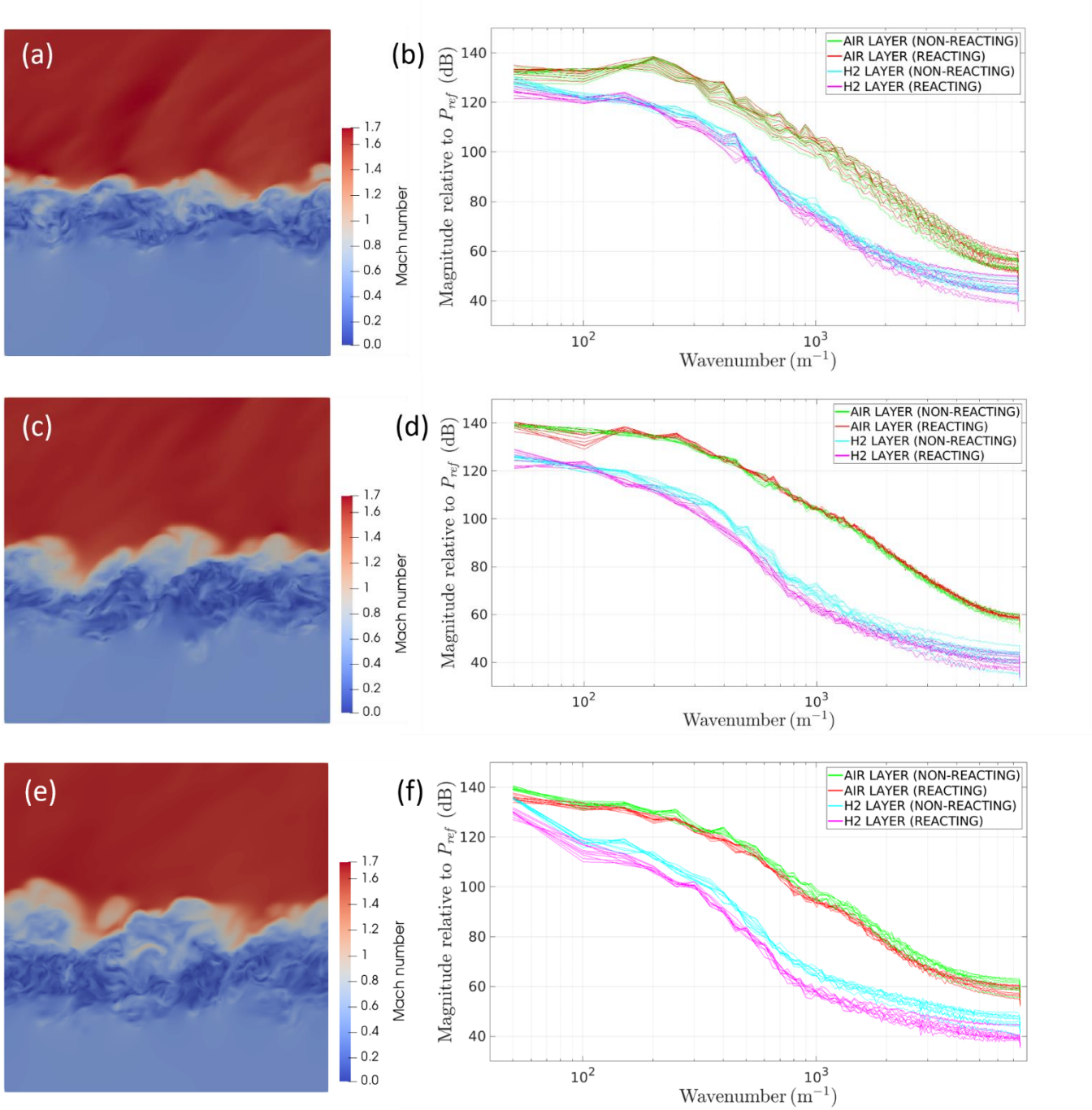

Figure 3. (a),(c),(e) Mach number contours of reacting flow at $Re_{\delta_\omega} \approx 8000$, 10500 and 12000 respectively; (b),(d),(f) corresponding PSD plots of pressure signal in air and hydrogen layers for reacting and non-reacting cases across 10 time points over Re_{δ_ω} range ≈ 1000.

sound waves generated by the mixing layer are coupling more readily with air than they are with hydrogen. In this early phase of the simulation, there is no clear difference between the spectra magnitudes for the reacting and non-reacting cases in either fluid. The dominant peak at wavenumber ≈ 200 in the spectra for the air layer appears to correspond to the distance between the initial large turbulent structures evident in the mixing layer, from which the strong Mach wave radiation seen in figure 2(b) originates.

Figures 3(c) and 3(d) show the equivalent flow visualization and pressure fluctuation plots at a later point in the simulation when $Re_{\delta_\omega} \approx 10500$. It can be seen that the magnitudes of the fluctuations in the air and hydrogen layers have further diverged, particularly at low wavenumbers. In the air layer, there is again no clear difference between the reacting and non-reacting cases. However, in the hydrogen layer, for wavenumbers between approximately 150 and 2000, the magnitudes of the pressure fluctuations appear consistently larger in the non-reacting case.

Finally, figures 3(e) and 3(f) correspond to the state of the flow near the end of the simulation at $Re_{\delta_\omega} \approx 12000$. Here the separation between the pressure plots in the air and hydrogen layers remains similar to that seen in figures 3(c) and 3(d), but the non-reacting flow now appears to be generating larger pressure fluctuations than the reacting flow in both fluid layers and at all wavenumbers. This is an unexpected result, and suggests the existence of some larger competing effect which is outweighing the sound generated by the turbulent combustion. One possible explanation may be that the turbulent growth rate of the mixing layer, and thus the production of sound by the turbulent mixing process, is being suppressed by the heat release from the combustion process [5].

Shortly beyond this point in the simulation, large convective pressure fluctuations resulting from the growing turbulent region start to encroach upon the lower observation slice and contaminate the acoustic signals of interest.

It may be noted that, due to the short simulation duration, the wavenumber resolution in figure 3 is quite coarse ($\sim 50\ m^{-1}$). As a result, it is difficult to discern very low-frequency sound with this type of analysis. This in turn means, for example, that we are unlikely to identify noise that may excite the structural modes of a scramjet engine. Identifying the high-frequency noise profile is nevertheless a valuable exercise, particularly in the context of identifying a fatigue risk that depends on the number of vibration cycles. In any event, the short test times ($\sim 2\ ms$) available in the University of Queensland's T4 reflected shock tunnel, under realistic scramjet test flight conditions, will also limit the frequency resolution of any experimental studies that may later be used to validate the computational model.

Conclusions

In this paper, we have explored via DNS the generation and propagation of acoustic pressure fluctuations from a supersonic reacting hydrogen-air mixing layer. Our results indicate that the sound waves emanating from the mixing layer do not propagate uniformly through the air and hydrogen layers, but appear to be coupling more readily with the air than the hydrogen, resulting in the hydrogen layer effectively being a quieter region of the flow. In addition, the non-reacting simulations appear to be producing more sound overall than the equivalent reacting cases. This suggests that the expected increase in sound production due to turbulent heat release in the reacting case is being suppressed or outweighed by some competing effect in the development of the turbulent flow. This is possibly caused by a reduction in the turbulent growth rate, and therefore in the noise produced by turbulent mixing, due to the heat release from the hydrogen combustion. These results may have important practical implications for scramjet design, and warrant further research.

Acknowledgements

The authors acknowledge with thanks Professor Graham Candler and his research group for providing access to the US3D solver.

This research was supported by the Australian Government through the Australian Research Council's *Discovery Projects* funding scheme (project DP170101105).

This research was undertaken with the assistance of resources and services from the National Computational Infrastructure (NCI), which is supported by the Australian Government.

References

[1] Dimotakis, P.E., The mixing transition in turbulent flows, *Journal of Fluid Mechanics*, vol. 409, 2000, 69-98.

[2] Ducros, F. *et al.*, Large-Eddy Simulation of the Shock/Turbulence Interaction, *Journal of Computational Physics*, vol. 152, no. 2, 1999, 517-549.

[3] Eason, T.G. & Spottswood, S., A Structures Perspective on the Challenges Associated with Analyzing a Reusable Hypersonic Platform, in *54th AIAA/ASME/ASCE/AHS/ ASC Structures, Structural Dynamics, and Materials Conference*, AIAA, 2013.

[4] Gibbons, N., Wheatley, V., & Doolan, C., Preliminary Investigation of Sound Generation in Scramjets, presented at the 20th Australasian Fluid Mechanics Conference, Perth, Australia, 5-8 December 2016.

[5] Hermanson, J.C. & Dimotakis, P.E., Effects of heat release in a turbulent, reacting shear layer, *Journal of Fluid Mechanics*, vol. 199, 2006, 333-375.

[6] Jachimowski, C.J., An analysis of combustion studies in shock expansion tunnels, Tech. Rep. NASA 3224, 1992.

[7] McBride, B.J., Zehe, M.J., & Gordon, S., NASA Glenn coefficients for calculating thermodynamic properties of individual species, Tech. Rep. 211556, 2002.

[8] Nompelis, I., Drayna, T., & Candler, G., Development of a Hybrid Unstructured Implicit Solver for the Simulation of Reacting Flows Over Complex Geometries, in *34th AIAA Fluid Dynamics Conference*, AIAA, 2004.

[9] Pantano, C., Sarkar, S., & Williams, F.A., Mixing of a conserved scalar in a turbulent reacting shear layer, *Journal of Fluid Mechanics*, vol. 481, 2003, 291-328.

[10] Papamoschou, D. & Roshko, A., The compressible turbulent shear layer: An experimental study, *J. Fluid Mech.*, vol. 197, 1988, 453-477.

[11] Peterson, D.M., Boyce, R.R., & Wheatley, V., Simulations of Mixing in an Inlet-Fueled Axisymmetric Scramjet, *AIAA Journal*, vol. 51, no. 12, 2013, 2823-2832.

[12] Smart, M.K., How Much Compression Should a Scramjet Inlet Do?, *AIAA Journal*, vol. 50, no. 3, 2012, 610-619.

[13] Subbareddy, P.K. & Candler, G.V., A fully discrete, kinetic energy consistent finite-volume scheme for compressible flows, *J. Comput. Phys.*, vol. 228, no. 5, 2009, 1347-1364.

[14] Tam, C.K.W., Viswanathan, K., Ahuja, K.K., & Panda, J., The sources of jet noise: experimental evidence, *Journal of Fluid Mechanics*, vol. 615, 2008, 253-292.

[15] Wright, M.J., Candler, G.V., & Prampolini, M., Data-parallel lower-upper relaxation method for the Navier-Stokes equations, *AIAA Journal*, vol. 34, no. 7, 1996, 1371-1377.